Associations of PTEN and ERG with Magnetic Resonance þÿ Imaging Visibility and Assessment of Non organ Pathology and Biochemical Recurrence After Radical Prostatectomy

Eineluoto, Juho T.

2021-11

Eineluoto , J T , Sandeman , K , Pohjonen , J , Sopyllo , K , Nordling , S , Stürenberg , C , Malén , A , Kilpeläinen , T P , Santti , H , Petas , A , Matikainen , M , Pellinen , T , Järvinen , P , Kenttämies , A , Rannikko , A & Mirtti , T 2021 , ' Associations of PTEN and ERG with þÿ Magnetic Resonance Imaging Visibility and Assessment of Non organ-c and Biochemical Recurrence After Radical Prostatectomy ' , European Urology Focus , vol. 7 , no. 6 , pp. 1316-1323 . https://doi.org/10.1016/j.euf.2020.06.016

http://hdl.handle.net/10138/338132
https://doi.org/10.1016/j.euf.2020.06.016

The association of PTEN, ERG and MRI visibility and assessment of non-organ confined pathology and biochemical recurrence after radical prostatectomy

Juho T. Eineluoto[a,d] *, Kevin Sandeman[a,b], Joona Pohjonen[a], Konrad Sopyllo[a], Stig Nordling[b], Carolin Stürenberg[a], Adrian Malén[a,d], Tuomas P. Kilpeläinen[d], Henrikki Santti[d], Anssi Petas[d], Mika Matikainen[d], Teijo Pellinen[c], Petrus Järvinen[d], Anu Kenttämies[e], Antti Rannikko[a,d], Tuomas Mirtti[a,b]

[a] Research Program in Systems Oncology, University of Helsinki, Helsinki, Finland

[b] Department of Pathology, University of Helsinki and Helsinki University Hospital, Helsinki, Finland

[c] Institute for Molecular Medicine Finland (FIMM), University of Helsinki, Helsinki, Finland

[d] Department of Urology, University of Helsinki and Helsinki University Hospital, Helsinki, Finland

[e] HUS Medical Imaging Center Department of Diagnostic Radiology, University of Helsinki and Helsinki University Hospital, Helsinki, Finland

* Corresponding author. Department of Urology, University of Helsinki and Helsinki University Hospital. Haartmaninkatu 4, 00029 HUS, Helsinki, Finland.

Tel. +358 94711; Fax +358 947175500.

E-mail address: juho.eineluoto@gmail.com (J.T. Eineluoto).

Abstract

Background: Diagnosing clinically significant prostate cancer (PCa) is challenging. Biomarkers and multiparametric magnetic resonance imaging (MRI) may facilitate this.

Objective: The main objective was to determine the association between biomarkers PTEN and ERG to visible and invisible PCa lesions in MRI. Furthermore, clinical, MRI and biomarker–related data were integrated for prediction of non-organ confined (OC) PCa and biochemical recurrence (BCR) after radical prostatectomy (RP).

Design, Setting and Participants: A retrospective analysis of a population-based cohort of men with PCa who underwent a preoperative MRI and RP during 2014-2015 in Helsinki University Hospital was conducted (n=346). A tissue microarray corresponding to the MRI visible and invisible lesions in RP specimens was constructed and stained for PTEN and ERG.

Outcome Measurements and Statistical Analysis: Association of PTEN and ERG with MRI visible and invisible lesions was examined (Pearson's χ^2 test), and the significance to predict non-OC disease together with clinical and MRI parameters was determined (ROC AUC and logistic regression analyses). BCR prediction was analyzed in Kaplan-Meier and Cox proportional hazards analyses.

Results and Limitation: Patients with MRI invisible lesions (n=35) had less PTEN loss and ERG positive expression compared with patients (n=90) with MRI visible lesions (17.2% vs 43.3% [p=0.006]; 8.6% vs 20.0% [p=0.125]). Patients with invisible lesions had better, but not statistically significant, BCR-free survival probability in Kaplan-Meier (p=0.055). BCR (5.7% vs 21.1%;

p=0.039), extraprostatic extension (11.4% vs 44.6%; p<0.001), seminal vesicle invasion (0% vs 21.1%; p=0.003), and lymph node metastasis (0% vs 12.2%; p=0.033) rates differed between the groups in favor of patients with MRI invisible lesions. Biomarkers did not have an independent significant role in predicting non-OC disease or BCR. Relatively short follow-up period was a limitation.

Conclusion: PTEN loss, BCR and non-OC RP findings were more often encountered with MRI visible lesions.

Patient summary: Magnetic resonance imaging of the prostate misses some cancer lesions. MRI invisible lesions seem less aggressive when compared with MRI visible lesions.

Keywords: biomarkers, ERG, multiparametric MRI, PI-RADS, prostate cancer, PTEN, radical prostatectomy

Introduction

Prostate biopsies (Bx) may repeatedly miss clinically significant prostate cancer (csPCa) resulting in undersampling [1]. The indiscriminate testing for elevated PSA has resulted in detection of low-risk PCa lesions and possible overtreatment [2]. Due to the challenges in early diagnostics and risk stratification, there is unmet need for better tools in decision-making for individual patients.

Multiparametric magnetic resonance imaging of the prostate (MRI) is typically reported in a structured manner using Prostate Imaging Reporting and Data System (PI-RADS) [3]. MRI may miss up to 20% of tumor lesions, especially those small in size and low in grade [4–7]. Delineating the biological properties of the MRI invisible vs visible lesions is of clinical importance, and could further help risk stratify men suspected for PCa.

Biomarkers may offer help in PCa detection. Inactivating mutations of tumor suppressor gene phosphatase and tensin homolog (PTEN) drive PCa progression and associate with several clinical outcomes [8–11]. There is loss of PTEN in 18-42% of PCa patients, and it associates with Gleason Grade Group (GGG) upgrading in radical prostatectomy (RP), biochemical recurrence (BCR) after RP, activation of castration-resistance mechanisms in metastatic PCa during androgen deprivation therapy, and altogether worse prognosis of PCa compared to patients with intact PTEN [8,10,12,13]. Another biomarker that has aroused a lot of interest is ERG. Fusion of the androgen receptor-regulated transmembrane protease serine 2 (TMPRSS2) with proto-oncogene ERG activates transcriptional pathways that promote PCa development [9,12]. PTEN and ERG protein expression detected by immunohistochemistry (IHC) correlate to large extent with genomic changes [13–15]. ERG IHC positive expression is found in 36-78% of primary PCa [8–10,12,13]. TMPRSS2:ERG fusion is considered an earlier change than PTEN loss [9,12] There is still largely unexplained association between ERG and PTEN status in human PCa and, increasing evidence

indicates that PCa without ERG expression combined with PTEN loss have worse outcome [8,12,13,16]

The association between MRI and biomarkers has been addressed [17–20], but knowledge on the interrelation between PI-RADS and biomarkers is scarce. As the use of PI-RADS is recommended by guidelines, this interrelation should be further investigated [21].

Here, we studied whether biomarkers PTEN and ERG, as surrogates for tumor aggressiveness, are associated with the visibility of the PCa lesions in MRI. Also, biomarker expression in RP specimens was compared with preoperative MRI PI-RADS scores, BCR and preoperative imaging-based assessment of non-organ confined (OC) cancer.

Material and methods

The study was approved by the institutional Ethics Committee (386/13/03/02/2014). In total, 598 consecutive patients underwent robot-assisted laparoscopic prostatectomy (RALP) as their primary therapy at the Department of Urology in Helsinki University Hospital during the study period January 2014 through September 2015. An extended lymphadenectomy was performed in patients with GGG ≥3 or >5% risk of lymph node positive disease according to the Memorial Sloan Kettering nomogram [22]. A preoperative MRI was performed at urologist's discretion and was done for 387 patients, whereas 211 patients did not have a preoperative MRI, but the groups' demographics did not differ significantly (Table 1). When tumor location data, preoperative MRI and biomarker data were matched, 41 patients were excluded due to insufficiency of data. Finally, 346 patients were available for biomarker analysis. The cohort was further divided according to PCa visibility in MRI based on evaluation of the RP specimen: patients with MRI visible lesions only (n=90, Group A), patients with MRI visible and invisible lesions (n=221, Group B), and

patients with MRI invisible lesions only (n=35, Group C) (Figure 1, Table 2). MRI visible lesions were considered as PI-RADS score 3-5 lesion with corresponding cancer in RP histopathological analysis. MRI invisible lesions were considered as tumor lesions of >0.5cm3 in RP histopathological analysis and absence of corresponding tumor lesion in preoperative MRI (PI-RADS scores 0-2). Clinical variables of interest included preoperative PSA, age, and clinical stage as assessed by digital rectal examination.

MRI

A prostate MRI was done either at diagnosis or before RALP using a Philips Achieva 3.0T MRI scanner producing 3.0 mm-thick image slices. The parameters included T2-weighted imaging, diffusion-weighted imaging with apparent diffusion coefficient mapping, and dynamic contrast enhancement. Imaging and image interpretation followed the European Society of Urogenital Radiology Guidelines [3]. MRI data was systematically reported using PI-RADS version 1 including the number of lesions, tumor volume, and non-OC findings such as extraprostatic extension (EPE), seminal vesicle invasion (SVI), and lymph node metastasis (LNM).

RALP tissue microarray

After RP, formalin fixation and paraffin embedding of the prostate and LNs were performed at HUSLAB Laboratory services, HUS. The central parts of the prostate were mounted in horizontal, apex and basis in sagittal, and seminal vesicles in individual slices. Obturator and inguinal LNs were mounted separately from both sides. Diagnostic microscope slides were stained with hematoxylin and eosin (H&E) and areas selected for the tissue microarray (TMA) construction were punched with 1.0 mm puncher core according to annotations made by three uropathologists (KS, SN and TM). The TMA was designed as follows: three cores per each cancer focus representing the primary region of interest (ROI1) on the MRI, two cores per secondary and tertiary ROIs (ROI2 and

ROI3), and one adjacent benign core per each RP specimen for staining control. Additionally, all csPCa invisible lesions in the MRI were marked on the RP H&E slides, and the most significant missed lesion was punched into TMA, representing the MRI invisible lesion when applicable. From each TMA block, 4 µm-thick sections for H&E, PTEN and ERG staining were cut and mounted on electrically charged glass slides.

Immunohistochemistry

IHC staining was performed on TMA sections using an autostainer (Dako A/S, Glostrup, Denmark) as previously published [8]. In short, TMAs were deparaffinized, heated in a microwave oven for antigen retrieval, blocked for endogenous peroxidase and then incubated with 1:100 dilution for PTEN antibody (D4.3 XP; Cell Signaling Technology, Danvers, MA, USA), and 1:300 dilution for ERG antibody (EPR 3864; Abcam PLC, Cambridge, UK). Each slide was then digitalized using a Pannoramic P250 Flash II whole slide scanner (3DHistec, Budapest, Hungary) equipped with 20x objective producing a resolution of 0.33 µm/pixel.

Antibody scoring

A WebMicroscope digital microscope platform (FIMM, Helsinki, Finland) was used for visual scoring of the TMA sections for antibody staining by three individual observers (JE, KoS and TM). Inconsistencies were solved by consensus. Benign prostatic epithelium served as positive staining control for PTEN and endothelial cells for ERG. Cancer epithelial cell cytoplasmic PTEN expression was dichotomously interpreted as positive or negative in comparison to benign epithelium. Cancer epithelial cell nuclear ERG staining was compared to the endothelial cell nuclei and assessed as negative, low, intermediate or strong, and later for statistical purposes dichotomized as negative (negative or low) or positive (intermediate or strong). Scoring was performed in concordance with previous studies [8,15,16].

Statistical analysis

Pearson's χ^2 and Fisher's exact tests were used for comparing groups A, B and C (Table 2). Logistic regression including ROC AUC analysis, with MRI and clinical data before RALP as variables, was used to study a) non-OC findings in RP and b) BCR after RP. Kaplan-Meier survival curves for BCR (two consecutive PSA values above 0.2ng/ml after RALP) and Cox proportional hazards models were calculated. All statistical analyses were performed using R Statistical Software v.3.6.1 (R foundation for statistical Computing, Vienna, Austria) using the packages survival and mice. A p value of <0.05 was considered statistically significant.

Results

The full clinical, radiological and biomarker characteristics of the patients included in the study as well as a non-MRI RP cohort for comparison are presented in Table 1.

Our primary aim was to characterize the properties of MRI invisible vs visible lesions. Biologically, invisible lesions had less PTEN loss than visible lesions (17.2% vs 43.3%; p=0.006), which indicates a less aggressive behavior. ERG expression was more frequent in patients with MRI visible lesion(s) than in those with invisible lesion(s) (Group A 20.0%, Group B 11.3%, and Group C 8.6%), but these differences were not statistically significant (Table 2). As expected, we found that the invisible lesions had lower GGGs in RP and have less frequently spread beyond the prostate (Table 2).

Next, we studied whether the MRI characteristics are able to add to the clinical variables in predicting non-OC disease at RP. Additionally, we analyzed the impact of adding the biomarker status to the MRI and clinical parameters in adverse stage correlation. In ROC AUC analysis, we found that MRI has a significant additional role in predicting non-OC disease after RP (p=0.006,

Figure 2). The biomarker expression, however, does not improve the prediction significantly. In the multivariate logistic regression analysis, the clinical (preoperative PSA, age, cT ≥3) and MRI (any non-OC finding, prostate volume) variables significantly predicted non-OC disease, while PI-RADS ≥3, and ERG or PTEN expression status did not (Supplementary Table 1).

BCR was less common in patients with MRI invisible lesions only than in patients with MRI visible lesions only (5.7% vs 21.1%; p=0.039, Table 2). However, in survival analysis, BCR-free survival between Groups A (invisible lesions), B (invisible and visible lesions) and C (invisible lesions only) (p=0.093, Figure 3a) or between groups dichotomized as Group A (visible) versus Groups B+C (MRI invisible and additional ≥1 visible lesion) (p=0.055, Figure 3b) did not meet the consensus criteria for statistical significance. For comparison, the analysis was done also between patients with visible lesions (Groups A+B) vs. invisible lesions (Group C), but the difference was not significant (p=0.1, Figure 3c). In ROC AUC analysis for BCR prediction, there were significant differences between the clinical versus clinical and MRI data (p<0.001, Supplementary Figure 1). PTEN intact/loss or ERG negative/positive expression did not separate the patients into two groups with significantly different BCR-free survival curves on a patient-based (Figure 4) or lesion-based (Supplementary Figure 2) analysis, and neither were they associated with tumor volume individually or combined (Supplementary Figure 3). Cox proportional hazards models with the MRI visibility groupings (A vs B vs C; and A vs B+C) or the biomarker status were not significantly different from a model without these variables (data not shown).

All in all, compared to patients with MRI invisible lesions, patients with MRI true-positive lesions seem to harbor higher GGG, more BCR, more PTEN loss, and more non-OC findings, such as EPE, SVI and LNM.

Discussion

In this study, we found that PTEN staining was more often lost in MRI visible than invisible lesions. Furthermore, MRI invisible PCa lesions appeared less aggressive than MRI visible lesions in terms of high GGG, EPE, SVI, and LNM in RP. Also, BCR after RP was less common among the patients with MRI invisible lesions only. This suggests a less aggressive phenotype for MRI invisible lesions. Further, we evaluated the effect of MRI visibility on a more clinical end-point, i.e. BCR, and found that in Kaplan-Meier survival analysis with a median follow-up time of 3.3 years, MRI visibility was not statistically significantly related to BCR.

Evidence suggests that MRI invisible lesions are less aggressive than MRI visible lesions [4,5,23–27]. MRI most likely misses small (diameter 1-5mm), less aggressive (GGG 1), and multifocal nonindex lesions [25]. However, the prognostic significance and biological characteristics of these MRI invisible lesions are not yet fully understood. A recent study reported no difference in detection rates of csPCa among men who had ≥2 negative MRIs and who were divided into groups of Bx-naïve and prior negative Bx [28]. Also, a study of over 4200 men showed csPCa disease-free survival of 99.6% among men with only PI-RADS≤2 lesions [29]. In our study, we could not demonstrate a statistically significant difference in BCR-free survival analysis between PTEN, ERG, and MRI visibility (Supplementary Figure 2).

Biomarkers and MRI may aid in correctly defining csPCa. Lee et al. studied the biomarker characteristics of MRI visible and invisible lesions in a small cohort of 48 patients [7]. The two groups had different molecular characteristics with e.g. CHD1-deletions being present in only MRI invisible lesions while SPINK1-biomarker was not expressed in MRI invisible lesions. In their study, PI-RADS was retrospectively assigned. Li et al. analyzed the differences in gene expression of MRI visible and MRI invisible lesions [30]. Gene expression profile in MRI invisible tumors was

associated with better PCa prognosis and the result was not fully explained by GGG or tumor volume. Also, MRI invisible lesions have been shown to have lower risk for early metastasis than MRI visible lesions in the commercially available Decipher® gene panel [27]. Likewise, MRI visible tumors are enriched with genes of increased mutational burden and higher prevalence of cribriform architecture [4]. Thus, MRI lesion visibility associates with its biological behavior. All these studies, however, suffer from small cohort sizes and short follow-up time.

In our study, MRI visible lesions tended to progress faster based on the Kaplan-Meier survival analysis, albeit the common criteria for statistical significance were not reached. When compared with the other clinical parameters, MRI visibility as an independent prognostic factor for BCR could not be established. Literature suggests that PCa lesions with ERG negative and PTEN loss expression seem to progress faster [8,13]. ERG rearrangement is reported to occur in 36-78%, and PTEN loss in 18-42% of PCa cases [8–10]. Here, we showed ERG rearrangement in 14% (28/205) in MRI invisible lesions and 27% (80/299) in MRI visible lesions. Also, we showed a rate of PTEN loss of 15% (28/192) in MRI invisible lesions and 39% (113/292) in MRI visible lesions. Our data is in line with the literature. Likely due to lack of follow-up time and limited number of patients, PTEN and ERG expressions showed no added benefit in logistic regression analysis or Kaplan-Meier survival analysis.

Limitations of the study include relatively small number of patients with only MRI invisible or only MRI visible lesions, relatively short follow-up time, and lack of a validation cohort. Furthermore, as the PI-RADS recommendations were first published in 2012, the inherent deduction is that PI-RADS era cohorts with long enough follow-up time to study definitive clinical end-points, such as PCa specific mortality, do not exist.

Strengths of the study include a large cohort consisting of all RP patients in non-tertiary referral hospitals and no obvious bias for MRI selection as illustrated in Table 1. Also, using RP whole-mount pathology as a control for MRI findings, and matching the histopathological findings exactly using PI-RADS, allows for detailed analysis of the biology of the MRI invisible vs visible lesions.

Future studies are needed to elucidate the use of combined biomarker and MRI data for prediction of PCa behavior. Whether MRI invisible lesions are clinically as significant as their MRI visible counterparts needs to be addressed in studies with long-term follow-up after negative MRI. To fully elucidate the full clinical potential of biomarkers, such as PTEN and ERG, in conjunction with MRI should ideally be evaluated already at diagnosis using biopsies as a source for tissue and expanding the cohorts to include lower-risk PCa.

Conclusions

Our results suggest that false-negative MRI lesions, as judged by their biomarker status, may not be as aggressive as true-positive MRI lesions. This adds to the debate on whether systematic biopsies are needed in men with negative prebiopsy MRI.

Acknowledgements

Orion Research Foundation sr, Cancer Foundation Finland, Finnish-Norwegian Medical Foundation and Ida Montin Foundation funded this research.

References

[1] Lahdensuo K, Mirtti T, Petas A, Rannikko A. Performance of transrectal prostate biopsies in detecting tumours and implications for focal therapy. Scand J Urol 2015;49:90-6.

[2] Arnsrud Godtman R, Holmberg E, Lilja H, Stranne J, Hugosson J. Opportunistic testing versus organized prostate-specific antigen screening: outcome after 18 years in the Göteborg randomized population-based prostate cancer screening trial. Eur Urol 2015;68:354-60.

[3] Barentsz JO, Richenberg J, Clements R, et al. ESUR prostate MR guidelines 2012. Eur Radiol 2012;22:746–57.

[4] Houlahan KE, Salmasi A, Sadun TY, et al. Molecular hallmarks of multiparametric magnetic resonance imaging visibility in prostate cancer. Eur Urol 2019;76:18-23.

[5] van Houdt PJ, Ghobadi G, Schoots IG, et al. Histopathological features of MRI-Invisible regions of prostate cancer lesions. J Magn Reson Imaging 2019;51:1235-46.

[6] Le JD, Tan N, Shkolyar E, et al. Multifocality and prostate cancer detection by multiparametric magnetic resonance imaging: correlation with whole-mount histopathology. Eur Urol 2015;67:569-76.

[7] Lee D, Fontugne J, Gumpeni N, et al. Molecular alterations in prostate cancer and association with MRI features. Prostate Cancer Prostatic Dis 2017;20:430-5.

[8] Lahdensuo K, Erickson A, Saarinen I, et al. Loss of PTEN expression in ERG-negative prostate cancer closepredicts secondary therapies and leads to shorter disease-specific survival time after radical prostatectomy. Mod Pathol 2016;29:1565-74.

[9] Boström PJ, Bjartell AS, Catto JW, et al. Genomic predictors of outcome in prostate cancer. Eur Urol 2015 Dec;68:1033-44.

[10] Lokman U, Erickson AM, Vasarainen H, Rannikko AS, Mirtti T. PTEN loss but not ERG expression in diagnostic biopsies is associated with increased risk of progression and adverse surgical findings in men with prostate cancer on active surveillance. Eur Urol Focus 2017;4:867-73.

[11] Mithal P, Allott E, Gerber L, et al. PTEN loss in biopsy tissue predicts poor clinical outcomes in prostate cancer. Int J Urol 2014;21:1209-14.

[12] Ullman D, Dorn D, Rais-Bahrami S, Gordetsky J. Clinical utility and biologic implications of phosphatase and tensin homolog (PTEN) and ETS-related gene (ERG) in prostate cancer. Urology 2018;113:59-70.

[13] Haney NM, Faisal FA, Lu J, et al. PTEN loss with ERG negative status is associated with lethal disease after radical prostatectomy. J Urol 2020;203:344-50.

[14] Chaux A, Albadine R, Toubaji A, et al. Immunohistochemistry for ERG expression as a surrogate for TMPRSS2-ERG fusion detection in prostatic adenocarcinomas. Am J Surg Pathol 2011;35:1014-20.

[15] Lotan TL, Gurel B, Sutcliffe S, et al. PTEN protein loss by immunostaining: analytic validation and prognostic indicator for a high risk surgical cohort of prostate cancer patients. Clin Cancer Res 2011;17:6563-73.

[16] Ahearn TU, Pettersson A, Ebot EM, et al. A prospective investigation of PTEN loss and ERG expression in lethal prostate cancer. J Natl Cancer Inst 2016;108.

[17] Renard Penna R, Cancel-Tassin G, Comperat E, et al. Apparent diffusion coefficient value is a strong predictor of unsuspected aggressiveness of prostate cancer before radical prostatectomy. World J Urol 2016;34:1389-95.

[18] VanderWeele DJ, Turkbey B, Sowalsky AG. Precision management of localized prostate cancer. Expert Rev Precis Med Drug Dev 2016;1:505-15.

[19] McCann SM, Jiang Y, Fan X, et al. Quantitative Multiparametric MRI Features and PTEN Expression of Peripheral Zone Prostate Cancer: A Pilot Study. AJR Am J Roentgenol 2016;206:559-65.

[20] Lee D, Fontugne J, Gumpeni N, et al. Molecular alterations in prostate cancer and association with MRI features. Prostate Cancer Prostatic Dis 2017;20:430-5.

[21] Mottet N, Bellmunt J, Bolla M, et al. EAU-ESTRO-SIOG Guidelines on prostate cancer. Part 1: screening, diagnosis, and local treatment with curative intent. Eur Urol 2017;71:618-29.

[22] Ohori M, Kattan MW, Koh H, et al. Predicting the presence and side of extracapsular extension: a nomogram for staging prostate cancer. J Urol 2004;171:1844-9.

[23] Rosenkrantz AB, Mendrinos S, Babb JS, Taneja SS. Prostate cancer foci detected on multiparametric magnetic resonance imaging are histologically distinct from those not detected. J Urol 2012;6:2032-8.

[24] Lee MS, Moon MH, Kim YA, et al. Is Prostate Imaging Reporting and Data System Version 2 sufficiently discovering clinically significant prostate cancer? Per-lesion radiology-pathology correlation study. AJR Am J Roentgenol 2018;211:114-20.

[25] Johnson DC, Raman SS, Mirak SA, et al. Detection of individual prostate cancer foci via multiparametric magnetic resonance imaging. Eur Urol 2019;75:712-20.

[26] Dianat SS, Carter HB, Pienta KJ, et al. Magnetic resonance-invisible versus magnetic resonance-visible prostate cancer in active surveillance: a preliminary report on disease outcomes. Urology 2015;85:147-53.

[27] Purysko AS, Magi-Galluzzi C, Mian OY, et al. Correlation between MRI phenotypes and a genomic classifier of prostate cancer: preliminary findings. Eur Radiol 2019;29:4861-70.

[28] Panebianco V, Barchetti G, Simone G, et al. Negative multiparametric magnetic resonance imaging for prostate cancer: What's next?. Eur Urol 2018;74:48-54.

[29] Venderink W, van Luijtelaar A, van der Leest M, et al. Multiparametric magnetic resonance imaging and follow-up to avoid prostate biopsy in 4259 men. BJU Int 2019;124:775-84.

[30] Li P, You S, Nguyen C, et al. Genes involved in prostate cancer progression determine MRI visibility. Theranostics 2018;8:1752-65.

Figure 1

Flowchart of the study population.

MRI: magnetic resonance imaging; PI-RADS: prostate imaging reporting and data system

Figure 2

Prediction of non-organ confined disease at radical prostatectomy histopathological analysis. ROC AUC analysis with DeLong's test for significance between different groups of variables.

Figure 3

Kaplan-Meier curves for biochemical recurrence-free survival between the groups with different mpMRI visibility of prostate cancer lesions.

a.) Groups A vs B vs C.

b.) Groups A vs B + C.

c.) Groups A + B vs C.

Group A = mpMRI visible lesions only, n=90.

Group B = mpMRI visible and invisible lesions, n=218.

Group C = mpMRI invisible lesions only, n=35

Figure 4

Kaplan-Meier curves for biochemical recurrence-free survival between the groups with different biomarker status.

a.) PTEN intact/loss

b.) ERG positive/negative

Supplementary figure 1

Prediction of biochemical recurrence after radical prostatectomy. ROC AUC analysis with DeLong's test for significance between different groups of variables.

Supplementary figure 2

Kaplan-Meier curves for biochemical recurrence-free survival between the groups with different PTEN and ERG expression.

a.) PTEN intact/loss staining in mpMRI visible lesions.

b.) PTEN intact/loss staining in mpMRI invisible lesions

c.) ERG positive/negative staining in mpMRI visible lesions.

d.) ERG positive/negative staining in mpMRI invisible lesions.

mpMRI: multiparametric magnetic resonance imaging; ROI = region of interest

Supplementary figure 3

Box plot analysis of tumor volume and PTEN, ERG and MRI visibility.

a.) Solitary biomarkers

b.) Combined biomarkers

Table 1. Patient characteristics of a RP cohort with and without a preoperative MRI.

	Preoperative MRI (n=346)		No preoperative MRI (n=211)	
	Result	**% of total/IQR**	**Result**	**% of total/ IQR**
Median age, yr	65	60-69	66	61-70
Median preoperative PSA, ng/ml	8.9	6.2-13.0	8.3	3.6-9.9
Biochemical recurrence	52	15	NA	NA
Lymph node dissection performed	158	46	79	37
Gleason Grade Group at RP				
1	14	4.0	11	5.3
2	138	40	89	42
3	153	44	78	37
4	10	3.0	8	3.8
5	31	9.0	20	9.5
Data missing	-	-	5	2.4
Pathological stage at RP				
≤pT2	207	60	124	59
Seminal vesicle infiltration	41	12	18	8.5
Extraprostatic extension	137	40	79	37
Lymph node metastasis	21	6.1	17	8.1
PTEN, visible lesions (n=311) *				
Intact	179	58	-	-
Loss	113	36	-	-
NA or data missing	19	6.1		
PTEN, invisible lesions (n=256) *				
Intact	164	64	-	-
Loss	28	11	-	-
NA or data missing	64	25		
ERG, visible lesions (n=311) *				
Negative	219	70	-	-
Positive	80	26	-	-
NA or data missing	12	3.9		
ERG, invisible lesions (n=256) *				
Negative	177	69	-	-
Positive	28	11	-	-
NA or data missing	51	20		

IQR = interquartile range; RP = radical prostatectomy; * All patients did not have both visible and invisible lesions.

420

acteristics of RP patients in MRI visible and MRI invisible groups, and characteristics of tumor lesions between groups (n=346)

	A: Only visible lesions, n = 90		B: Visible and invisible lesions, n = 221		C: Only invisible lesions, n = 35		A vs B	*p val* B vs C
	Result	**IQR/% of total**	**Result**	**IQR/% of total**	**Result**	**IQR/% of total**		
	65	60 - 69	65	60 - 69	61	55 - 65	0.8[c]	**0.001[c]**
ative PSA, ng/ml	10.0	6.5 - 16	8.4	6.3 - 12	7.1	5.2 - 11	0.08[c]	0.1[c]
urrence	19	21	31	14	2	5.7	0.1[a]	0.3[b]
Group at RP								
	1	1.1	5	2.3	8	23	0.7[b]	**<0.001[b]**
	30	33	90	41	18	51	0.2[a]	0.2[a]
	38	42	107	48	8	23	0.3[a]	**0.005[a]**
	4	4.4	6	2.7	0	0	0.5[a]	1[b]
	17	19	13	5.9	1	2.8	**0.001[a]**	0.7[b]
ge at RP								
	49	55	127	58	31	89	0.6[a]	**<0.001[a]**
tatic extension	41	46	92	42	4	11	0.5[a]	**0.001[a]**
esicle infiltration	19	21	22	10	0	0	**0.008[a]**	0.052[b]
ode metastasis	11	12	10	4.5	0	0	**0.014[a]**	0.4[b]
esions (n=311)								
	50	56	129	58	–	–	0.6[a]	NA
	39	43	74	34	–	–	0.1[a]	NA
a missing	1	1.1	18	8.1	–	–	NA	NA
lesions (n=256)								
	–	–	139	63	25	71	NA	0.3[a]
	–	–	22	10	6	17	NA	0.2[a]
a missing	–	–	60	27	4	11	NA	NA
ions (n=311)								
	72	80	147	67	–	–	**0.018[a]**	NA
	18	20	62	28	–	–	0.1[a]	NA
a missing	–	–	12	5.4	–	–	NA	NA
esions (n=256)								
	–	–	148	67	29	83	NA	0.059[a]
	–	–	25	11	3	8.6	NA	0.6[a]
a missing	–	–	48	22	3	8.6	NA	NA

b Fisher's exact; c Mann-Whitney U; IQR = interquartile range; RP = radical prostatectomy

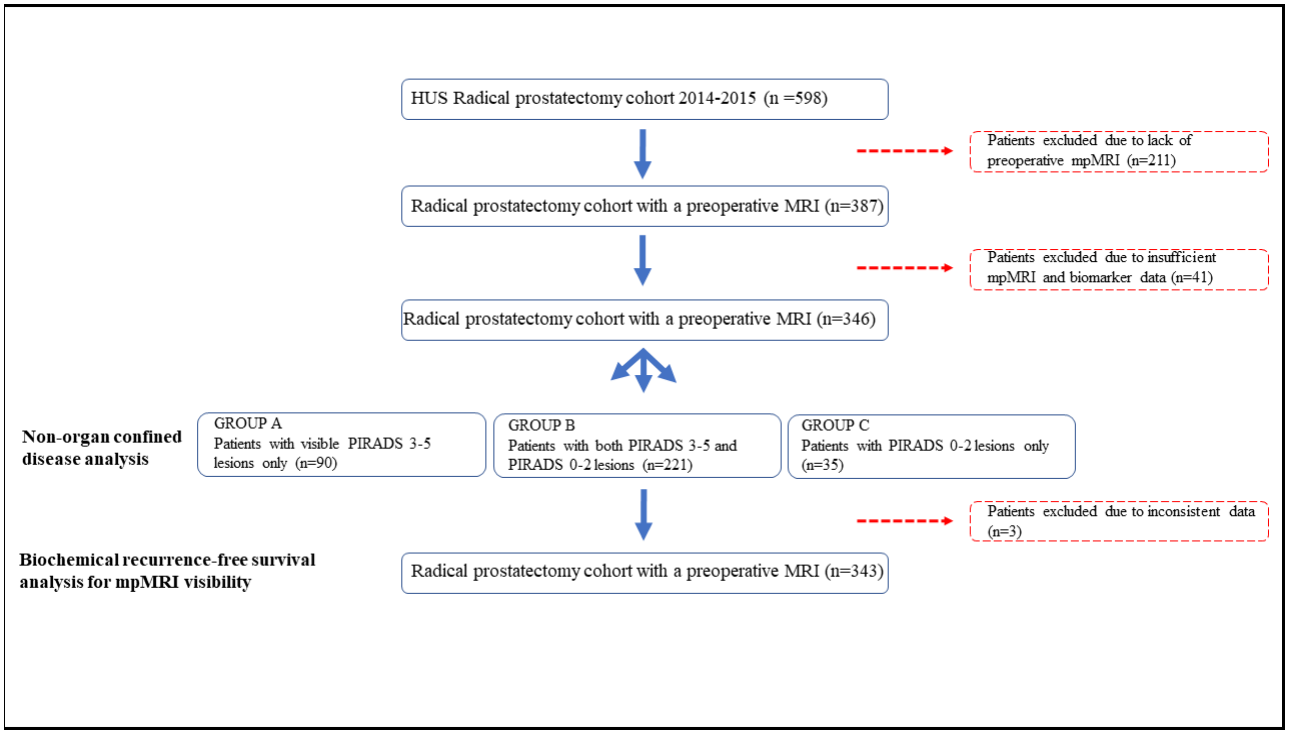
HUS Radical prostatectomy cohort 2014-2015 (n =598)
Patients excluded due to lack of preoperative mpMRI (n=211)
Radical prostatectomy cohort with a preoperative MRI (n=387)
Patients excluded due to insufficient mpMRI and biomarker data (n=41)
Radical prostatectomy cohort with a preoperative MRI (n=346)
Non-organ confined disease analysis
GROUP A
Patients with visible PIRADS 3-5 lesions only (n=90)
GROUP B
Patients with both PIRADS 3-5 and PIRADS 0-2 lesions (n=221)
GROUP C
Patients with PIRADS 0-2 lesions only (n=35)
Patients excluded due to inconsistent data (n=3)
Biochemical recurrence-free survival analysis for mpMRI visibility
Radical prostatectomy cohort with a preoperative MRI (n=343)

Figure 1

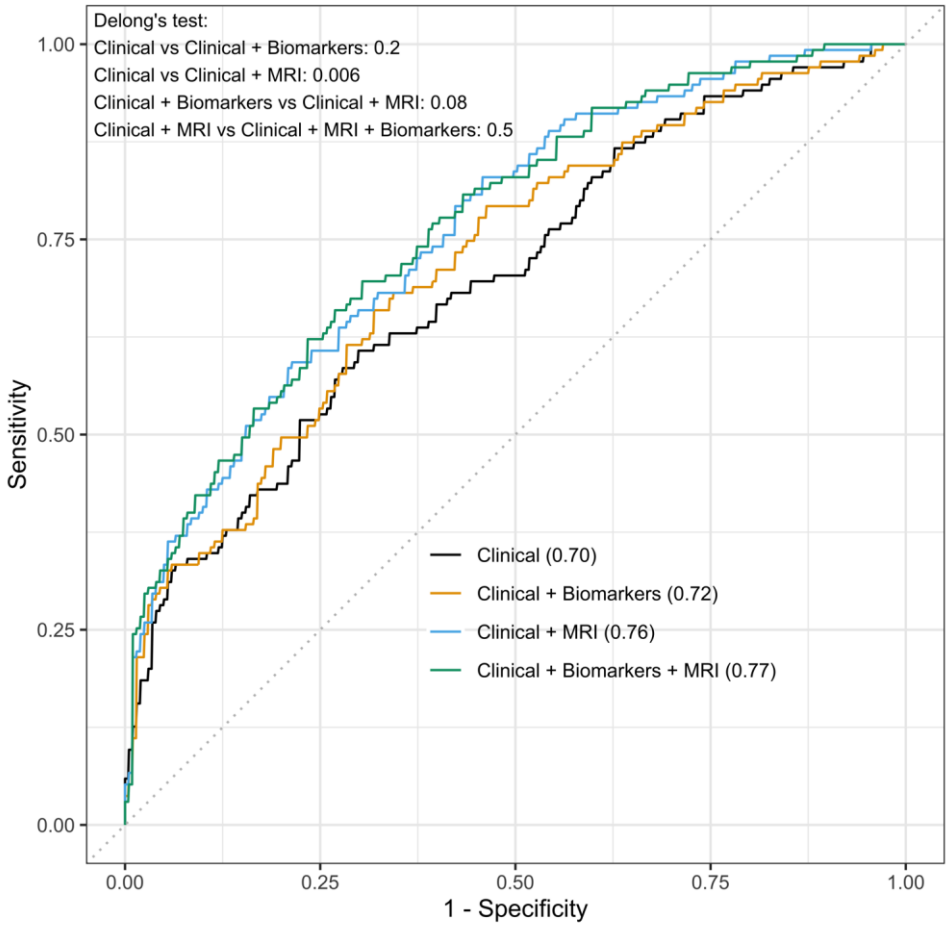
Delong's test:
Clinical vs Clinical + Biomarkers: 0.2
Clinical vs Clinical + MRI: 0.006
Clinical + Biomarkers vs Clinical + MRI: 0.08
Clinical + MRI vs Clinical + MRI + Biomarkers: 0.5
Clinical (0.70)
Clinical + Biomarkers (0.72)
Clinical + MRI (0.76)
Clinical + Biomarkers + MRI (0.77)
Sensitivity
1 - Specificity
0.00
0.25
0.50
0.75
1.00

Figure 2

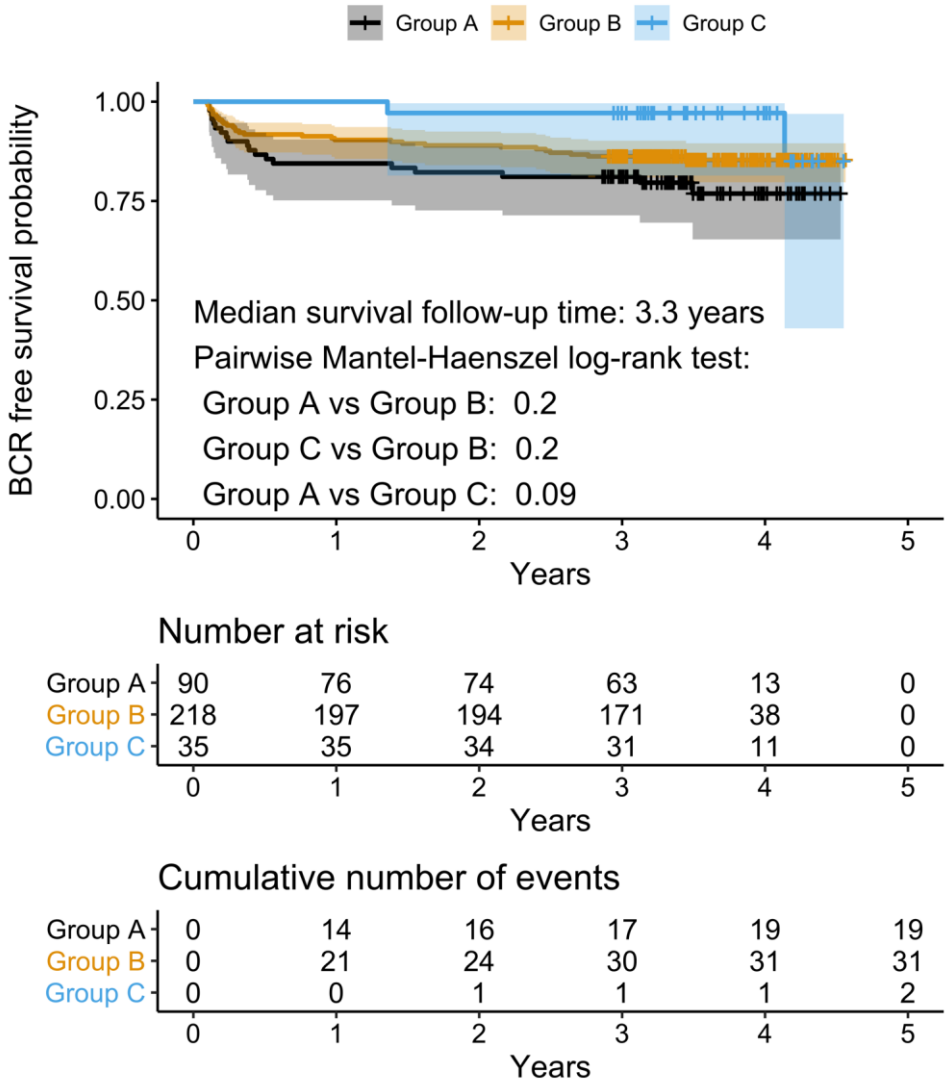
Group A
Group B
Group C
BCR free survival probability
1.00
0.75
0.50
0.25
0.00
Median survival follow-up time: 3.3 years
Pairwise Mantel-Haenszel log-rank test:
Group A vs Group B: 0.2
Group C vs Group B: 0.2
Group A vs Group C: 0.09
0
1
2
3
4
5
Years
Number at risk
Group A 90 76 74 63 13 0
Group B 218 197 194 171 38 0
Group C 35 35 34 31 11 0
Years
Cumulative number of events
Group A 0 14 16 17 19 19
Group B 0 21 24 30 31 31
Group C 0 0 1 1 1 2
Years

Figure 3a

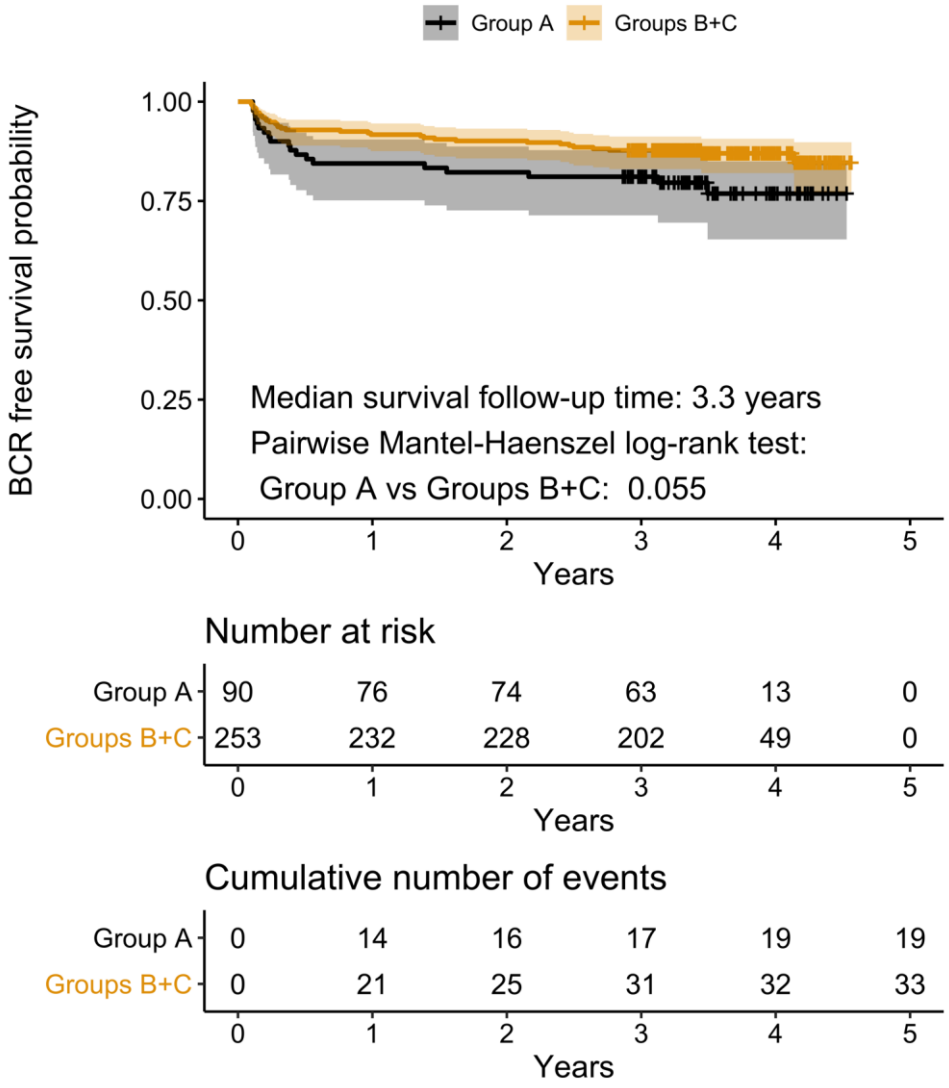
Group A
Groups B+C
BCR free survival probability
1.00
0.75
0.50
0.25
0.00
Median survival follow-up time: 3.3 years
Pairwise Mantel-Haenszel log-rank test:
Group A vs Groups B+C: 0.055
0
1
2
3
4
5
Years
Number at risk
Group A 90 76 74 63 13 0
Groups B+C 253 232 228 202 49 0
Cumulative number of events
Group A 0 14 16 17 19 19
Groups B+C 0 21 25 31 32 33

Figure 3b

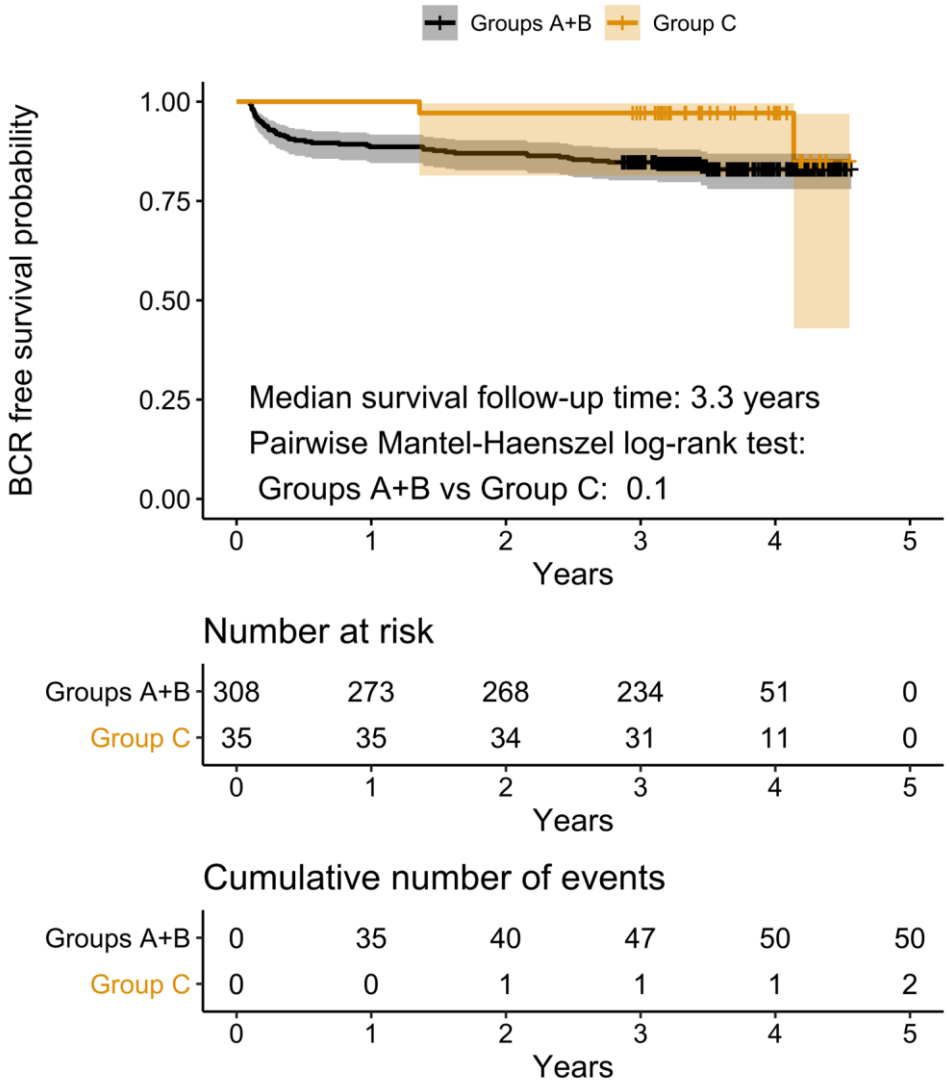
Groups A+B
Group C
BCR free survival probability
1.00
0.75
0.50
0.25
0.00
Median survival follow-up time: 3.3 years
Pairwise Mantel-Haenszel log-rank test:
Groups A+B vs Group C: 0.1
0
1
2
3
4
5
Years
Number at risk
Groups A+B 308 273 268 234 51 0
Group C 35 35 34 31 11 0
Years
Cumulative number of events
Groups A+B 0 35 40 47 50 50
Group C 0 0 1 1 1 2
Years

Figure 3c

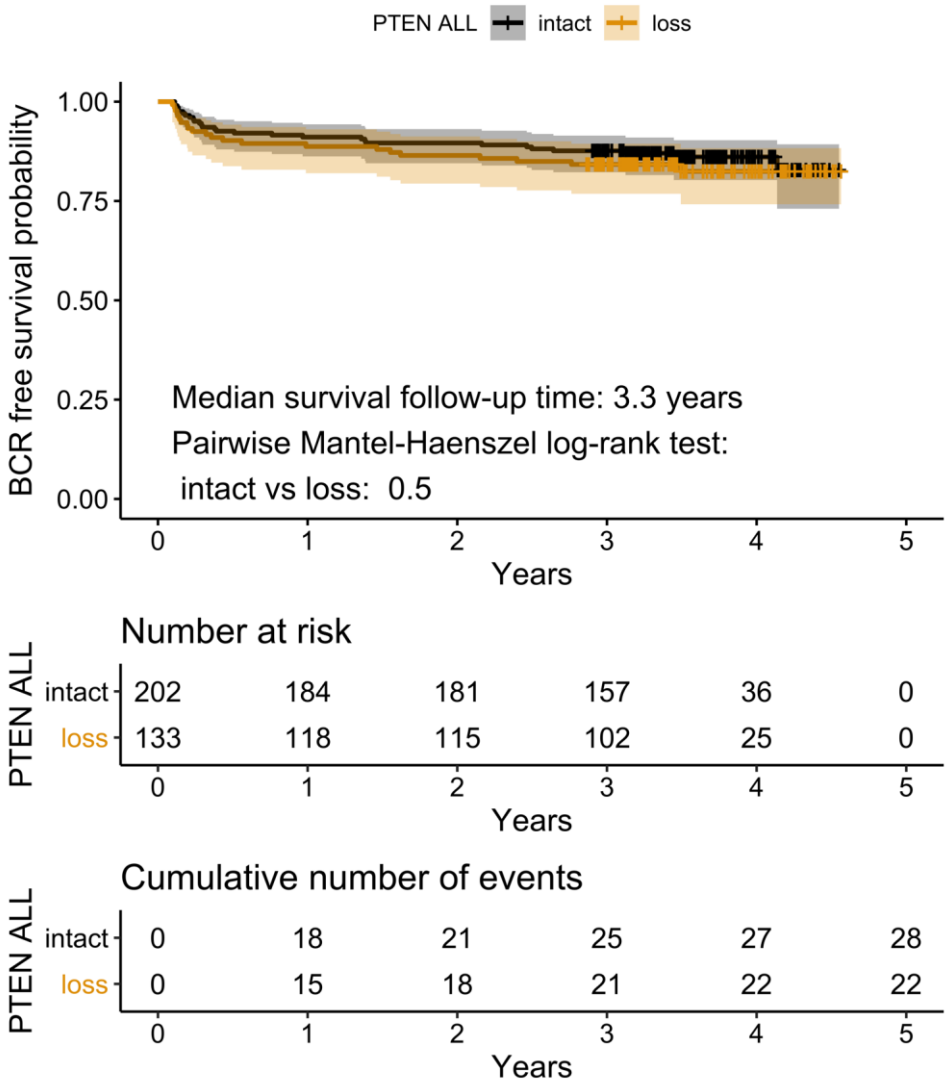
PTEN ALL
intact
loss
BCR free survival probability
1.00
0.75
0.50
0.25
0.00
Median survival follow-up time: 3.3 years
Pairwise Mantel-Haenszel log-rank test:
intact vs loss: 0.5
0
1
2
3
4
5
Years
Number at risk
PTEN ALL
intact 202 184 181 157 36 0
loss 133 118 115 102 25 0
Cumulative number of events
intact 0 18 21 25 27 28
loss 0 15 18 21 22 22

Figure 4a

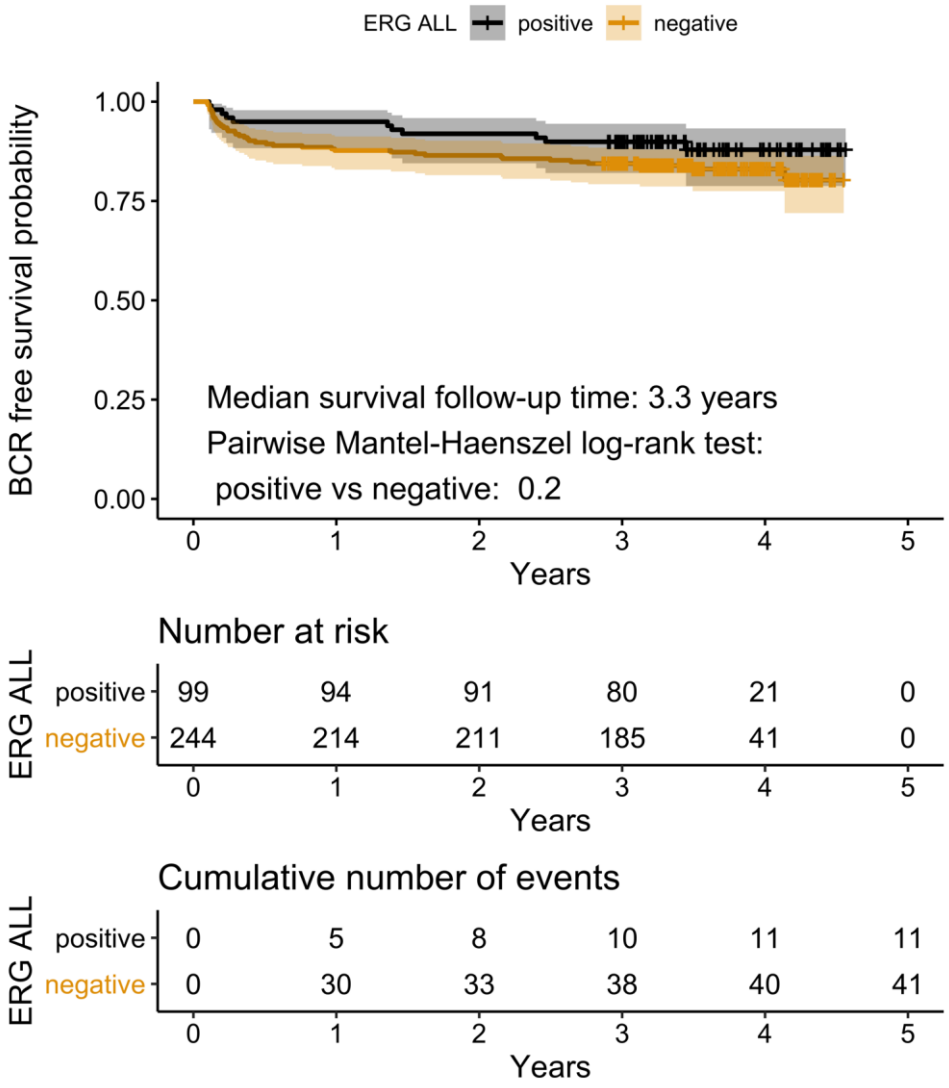
ERG ALL
positive
negative
BCR free survival probability
1.00
0.75
0.50
0.25
0.00
Median survival follow-up time: 3.3 years
Pairwise Mantel-Haenszel log-rank test:
positive vs negative: 0.2
0
1
2
3
4
5
Years
Number at risk
ERG ALL
positive 99 94 91 80 21 0
negative 244 214 211 185 41 0
Cumulative number of events
positive 0 5 8 10 11 11
negative 0 30 33 38 40 41

Figure 4b